Journal of Hydrospace Technology, Vol. 1, No. 2, 1995, pp. 59-68

A Nonlinear Calculation of 2-Dimensional Hydrofoill with Shallow Submergence

Seung-Joon Lee [1]

Abstract

For treating a hydrofoil moving with nonzero angle of attack, first, Tulin's theory[1] is extended, and some computational results are given. Then a newly developed source-vortex panel code, which employs a nonlinear free surface boundary condition proposed by Lee[2] and satisfies the Kutta condition, is explained, and its results are compared with the existing experimental data and other numerical results. Overall performance of the developed code is shown as satisfactory.

1 Introduction

Using a panel method(Douglas-Neumann type) to predict surface elevations resulting from a moving submerged hydrofoil, Van & Lee[3] compared various free surface boundary conditions(FSBC), and later Lee[2] proposed a nonlinear FSBC, which can be easily implemented in the numerical code. He showed that his FSBC gave better agreement than the commonly used Poisson or Dawson FSBC with the experimental measurements of Salvesen[4], however, there was still non-negligible difference between the computational prediction and the experimental data. A part of this difference was regarded as a result of not satisfying the Kutta condition at the trailing edge(TE) of the hydrofoil. In deriving his FSBC, Lee made use of the theory of Tulin[1], which is an exact theory(in the framework of potential theory) for predicting surface elevations due to moving submerged body. For obtaining computational results, Lee approximated Tulin's theory to the second order in a sense, and he restricted himself to those bodies, which have a longitudinal symmetric axis parallel to the incoming flow, and thus of which the angle of attack(AOA) is zero.

In this study, first, Tulin's theory is extended to include nonzero AOA cases, and some computational results are shown. Then to solve the flow field around a moving submerged hydrofoil with nonzero AOA we developed a source-vortex panel method, in which Lee's FSBC is implemented, and now the Kutta condition is satisfied. Numerical results are compared with the existing experimental data and other computational findings.

[1]Member,Dept. of Naval Architecture & Ocean Eng., Chungnam National University

2 Tulin's Theory - Extended to Nonzero AOA Cases

Tulin[1] proposed an exact theory of gravity wave generation by moving bodies, and its approximation, and part of his results can be summarized as follows.

For a submerged body in the incoming uniform flow of speed U, if we let $G = (\frac{d\Phi}{dz})^3 = q^3 e^{-3i\theta} = 1 + H$, where $\Phi = \phi + i\psi$ is the complex velocity potential corresponding to the unit velocity, q the modulus of the complex velocity, and θ its argument, then H is given as

$$H(\phi) = ie^{-i[K\phi - \alpha(\phi)]} \int_{-\infty}^{\phi} Q_i(\hat{\phi}) e^{i[K\hat{\phi} - \alpha(\hat{\phi})]} d\hat{\phi}, \tag{1}$$

where

$$\alpha(\phi) = \int_{-\infty}^{\phi} Q_i(\hat{\phi}) d\hat{\phi}, \tag{2}$$

and $K = {F_n}^{-2} = gL/U^2$(g is the gravitational acceleration, L the body length, F_n the Froude number). Here, Q_i represents the effect of the body and is given by

$$Q_i(\phi) = -6\frac{d\theta_s}{d\phi} + 2K(1 - \frac{\cos 3\theta_s}{q_s}), \quad \text{on } \psi = 0, \tag{3}$$

where the subscript s stands for the surrogate body. If we let Φ_s the complex velocity potential for the flow field around the surrogate body, and $\frac{d\Phi_s}{dz} = q_s e^{-i\theta_s}$, q_s and θ_s can be obtained as a function of Φ by,

$$\tau_s = \ln(q_s e^{-i\theta_s}) = \frac{1}{\pi} \int_0^1 \frac{\theta_u(\hat{\phi})}{\Phi - (\hat{\phi} - ih)} d\hat{\phi}, \tag{4}$$

where θ_u is the angle between the x-axis and the tangent of the upper surface of the hydrofoil in the physical z-plane(see figure 1). Once $H(\phi)$ is attained, we get the surface elevation by the transformation

$$z = \int \frac{d\phi}{(1+H)^{\frac{1}{3}}} = \int \frac{e^{i\theta}}{q} d\phi, \quad \text{on } \psi = 0. \tag{5}$$

In developing his theory, Tulin[1] neglected the circulatory motion around the body, and so did Lee[2]. However, as pointed out by Salvesen[5], for a foil-shaped body moving with high F_n the major part of the 'body-correction' comes from the effect of the circulatory motion, and truly it cannot be neglected for nonzero AOA cases. Although equations above were derived for the non-circulatory problem, it is believed that they are equally valid for the circulatory ones, since what has discontinuity or multi-valuedness is the velocity potential, not the velocity itself.

Now, for a hydrofoil moving in the infinite fluid domain, its lift can be said to consist of two parts. One is due to the camber, and the other due to the AOA. If we restrict ourselves to the symmetric foil only, we need not consider the camber effect. But for a hydrofoil moving under the free surface, in addition to the effect of AOA, that of the free surface must be included. For instance, a symmetric foil moving under the free surface with zero AOA experiences a lift, while the same foil in the infinite fluid does not. According to Kochin[6],

a moving submerged dipole of strength μ is acted upon lift Y, whose dimensionless form, $Y_d = Y/(\rho\mu^2/8\pi h^3)$ can be expressed as a function of $F_h = U/\sqrt{gh}$ alone(see figure 2), where ρ is the fluid density, and h the submerged depth. It is worthwhile to note that Y_d is positive for $F_h < 0.84$. We also note that this lift does not result from the Kutta condition, rather from the FSBC. However, Kochin obtained zero lift for a submerged flat plate with zero AOA due to his method of approximation, in which the Kochin function is used and for getting it the complex velocity on the body surface is replaced by that of the same body located in an infinite fluid. Of course, there is nonzero lift acting on the submerged symmetric hydrofoil with zero AOA, but for the thin hydrofoil it may be ignored as a first approximation.

To take the effect of AOA into account within the framework of Tulin's approach, first, we note that the treatment of Tulin explained above considers the 'thickness' problem only. We recall that the flow field around a symmetric thin hydrofoil with nonzero AOA in an infinite fluid is given by the sum of the source and the vortex distribution being the solution of the 'thickness' and the 'lifting' problem, respectively(see Newman[7]). Hence to satisfy the Kutta condition for the nonzero AOA case we need to add the 'vortex' distribution somehow to the original Tulin's solution. Since the complex velocity potential $\Phi_l(z)$ corresponding to the lifting problem for a thin hydrofoil may be expressed as follows,

$$\Phi_l(z) = -\frac{\alpha}{\pi i}\int_0^1 \sqrt{\frac{1-\xi}{\xi}}\ln[z-(\xi-ih)]d\xi, \tag{6}$$

where α is the AOA. And since as a first approximation we can regard $\Phi \sim z$, the complex velocity w_l as a function of Φ can then be given as

$$w_l(\phi) = -\frac{\alpha}{\pi i}\int_0^1 \sqrt{\frac{1-\hat{\phi}}{\hat{\phi}}}\frac{d\hat{\phi}}{\phi-(\hat{\phi}-ih)}, \quad \text{on } \psi = 0. \tag{7}$$

Using the first order solution for the lifting problem, while the second order one for the thickness problem, we can regard the present method as inconsistent second order accurate, and may expect the accuracy of the present method deteriorated compared to the non-circulatory cases. Regarding the complex velocity we obtain from (4) as w_t, the new q_s and θ_s, now including the effect of nonzero AOA, can be approximated by

$$q_s = |w_t + w_l|, \quad \theta_s = -\mathrm{Arg}(w_t + w_l). \tag{8}$$

To take care of the singular behavior of the integrand for w_l near the lower end point of the integration interval, we transform the integration variable using $2(\hat{\phi} - \frac{1}{2}) = \sin\beta$, then the integration can be easily carried out numerically, for instance, by the Simpson's rule.

To perform the example calculation, now we need only to specify θ_u in (4), and we used the same function as before in Lee[2], that is

$$\theta_u = -4\delta(\phi - \frac{1}{2}), \tag{9}$$

where δ can be understood as the maximum thickness of the body at $\phi = \frac{1}{2}$. In figure 3, taking $F_n = 0.4, \delta = 0.2, h = 1.0$, we compare $Q_i(\phi)$ when $\alpha = 0°, 1°, 3°$, and we

can clearly observe the trend of the increase in the magnitude of Q_i as α gets larger. In figure 4 we show the surface elevations for the same cases, and we confirm that the bigger Q_i results in the greater elevations. As α increases the free surface in front of the foil is lowered probably due to the circulatory motion around the foil. Although the method explained above cannot show what changes are made if we satisfy the Kutta condition for the zero AOA case, it is certainly effective in showing the mechanism of surface wave generation for nonzero AOA cases. All the wave-generating activity is represented by Q_i, which affects both the magnitude and the phase of the resulting wave system as shown up in (1).

3 Influence of Nonzero AOA on Surface Elevations & Pressure Distributions

In the previous work of Lee[2], various foil-shaped bodies of zero AOA were taken for example calculations, but the Kutta condition at the TE was not satisfied. This fact may have caused the difference between the numerical predictions and the experimental data. In order to describe the circulatory motion around the submerged body more properly, we developed a source-vortex panel code(a variation of Martensen-Dirichlet type) and used it instead of the source panel code(Douglas-Neumann type) adopted in the previous works. In coding for the treatment of the vortex panels the way described by Lewis[8] was most helpful. A few characteristics of the code are; a) On the body surface vortex panels are distributed, while on the undisturbed free surface source panels are distributed. b)Back diagonal correction for the vortex panels on the body is done to ensure that net circulation around the profile interior vanish. c)Wilkinson type Kutta condition is applied so that the strength of the vorticity distribution is the same for the two panels connected to TE, and the equation for the lower TE panel is deleted after it is subtracted from that for the upper one to make the linear system closed. d)Although the vorticity strength is assumed constant over a panel, and the panel shape rectilinear, the coupling coefficients(or influence coefficients) for the self-panel are corrected to take the effect of the change in the slope of the profile into account, which was first proposed by Lewis. e)In discretizing the FSBC, the 4-point upwind differencing used by Dawson[9] is adopted. And the mirror image of the body, having the vorticity strength of the equal magnitude but with the opposite sign to that of the body itself is also introduced to make the y-component velocity induced by the combination of the body and its image vanish on the line $y = 0$. Here, the velocity is non-dimensionalized by U, and the length by L.

The FSBC proposed by Lee[2] can be written as

$$(1 + 2\hat{u})u_x + (K + 2\hat{v}_x)v = 0, \quad \text{on } y = 0, \tag{10}$$

where the subscript stands for the partial differentiation, and $\underline{u} = (u, v), \underline{\hat{u}} = (\hat{u}, \hat{v})$ are the velocity vectors for the sought solution and the Poisson solution, respectively. Thus, $\underline{\hat{u}}$ satisfies the Poisson FSBC

$$\hat{u}_x + Kv = 0, \quad \text{on } y = 0. \tag{11}$$

Lewis[8] proposed a cambered Joukowski foil with smooth turning tangent at the TE, and we show in figure 5 the computational results for the Joukowski foil when $\alpha = 0°, h = 1.0, F_n = 0.4$. Here h is measured from the line $y = 0$ to the center-chord point. The pressure coefficient $C_p(= p/(\rho U^2/2))$, p being the pressure, for this case is compared with that of the foil in the infinite fluid for zero AOA and the unit speed. The value of $C_l = Y/(\rho U^2 L/2)$, the lift coefficient, for the submerged foil is 0.983, while that for the foil in the infinite fluid is 0.886. This shows that there is a range of parameters F_n and h, for which C_l increases due to the free surface effect.

For the Salvesen's foil, we compare the previous result, which was obtained without satisfying the Kutta condition, with the present one in figure 6, when $F_n = 0.422, \delta = 0.343, h = 0.9174, \alpha = 0°$, where δ is the maximum thickness. Although the foil, shown in figure 7 with other foils used in this study, is rather thick, the difference between two results are not notably big, which asserts our claim in the previous section. There is still some difference in surface elevations between the present result and the experimental data obtained by Salvesen[4]. Maybe the flow is highly nonlinear, and the second order correction accounted by the present method is not big enough for this particular case.

Though there are not many experimental measurements of the surface elevations generated by a hydrofoil with shallow submergence, Duncan[10] is one of such works. He towed a foil of the NACA 0012 section in a flume, and later Coleman[11] tried to simulate numerically the experimented cases with the finite difference code he developed. Duncan reported his measurements for various submerged depths, $h = 1.286, 1.162, 1.034, 0.951$, while AOA and F_n were kept constant, namely, $\alpha = 5°, F_n = 0.567$. In figure 8, we compare our results with Duncan's and Coleman's. As the submerged depth decreases, waveheights numerically obtained by the present method become larger, but not quite as much as those experimentally measured. Coleman's numerical values are greater than the experimental data, but our results smaller. Part of the difference may be due to effects of the bottom of the flume, which was taken into account in Coleman's calculation.

Parkin, Perry and Wu[12] is also one of the few experimental works on the pressure distribution on a hydrofoil, and they used the Joukowski symmetric foil with 12 % thickness. Their experimental cases also include a set, in which α and F_n are fixed, but h varied. Namely, $\alpha = 5°, F_n = 0.95$, while $h = 1.80, 1.0, 0.707$ (their h is defined as the distance from $y = 0$ to TE of the foil). We show in figure 9, the C_p curves predicted by the present method, compared with the experimental data. It is clear that for most cases agreement between two results is acceptable. But for some other cases of very shallow submergence, not shown here, there are still non-negligible differences between the improved numerical results and the experimental data. As Parkin et al. reported, wave breaking just behind the hydrofoil affected the flow field around the foil. But they did not make it clear in which cases of their measurements wave breaking occurred, so that it is hard to tell how the wave breaking alters the pressure distribution on the hydrofoil at this stage.

4 Conclusions

First, we showed a way to extend Tulin's theory[1] to include the effect of angle of attack in generating surface waves by moving submerged foil-shaped bodies. The extended theory

hinted us that how the circulatory motion around a foil affects the flow field and the surface waves. Then was introduced a newly developed source-vortex panel code, in which source panels are distributed on the undisturbed free surface, and vortex panels on the body surface. In coding, a nonlinear FSBC proposed by Lee[2] was also implemented, and the Kutta condition of the Wilkinson type was satisfied. Numerical results given by the code were compared with the experimental results of Salvesen[4], Duncan[10] and Parkin et al.[12], and with the numerical results of Coleman[11]. The agreement between the numerical and the experimental results are in general acceptable. But for future works it seems we need more experimental data of the surface waves and the pressure distribution on a hydrofoil measured for the same setting, so that we can clarify how the wave phenomena on the free surface affects the pressure distribution on the body surface.

References

[1] Tulin, M.P., "An exact theory of gravity wave generation by moving bodies, its approximation, and its implication," Proc. of 14th Symp. on Naval Hydro., 1982, pp. 19-51.

[2] Lee, S.J., "A practical method for computing wave resistance," Trans. of SNAK, Vol. 31, No. 1, Feb. 1994, pp. 111-120.

[3] Van, S.H. & Lee, S.J., "Comparison of free surface boundary conditions for computing wave resistance," Trans. of SNAK, Vol. 30, No. 2, May 1993, pp. 54-65.

[4] Salvesen, N., "On second-order wave theory for submerged two-dimensional bodies," Proc. of 6th Symp. on Naval Hydro., 1966, pp. 25:1-34.

[5] Salvesen, N., "On higher-order wave theory for submerged two-dimensional bodies," Journal of Fluid Mechanics, Vol. 38, Part 2, 1969, pp. 415-432.

[6] Kochin, N.E., "On the wave-making resistance and lift of bodies submerged in water," Technical & Research Bulletin No. 1-8, SNAME, 1951, pp. 1-126.

[7] Newman, J.N., *Marine Hydrodynamics*, MIT Press, 1977, pp. 159-236.

[8] Lewis, R.I., *Vortex Element Methods for Fluid Dynamic Analysis of Engineering Systems* , Cambridge Univ. Press, 1991, pp. 1-98.

[9] Dawson, C.W., "A practical computer method for solving ship-wave problems," Proc. of 2nd Int. Conf. on Num. Ship Hydro., 1977, pp. 30-38.

[10] Duncan, J.H., "The breaking and non-breaking wave resistance of a two-dimensional hydrofoil," Journal of Fluid Mechanics, Vol. 126, 1983, pp. 507-520.

[11] Coleman, R.M., "Nonlinear calculation of breaking and non-breaking waves behind a two-dimensional hydrofoil," Proc. of 16th Symp. on Naval Hydro., 1986, pp. 51-62.

[12] Parkin, B.R., Perry, B. and Wu, T.Y., "Pressure distribution on a hydrofoil running near the water surface," Journal of Applied Physics, Vol. 27, 1956, pp. 232-240.

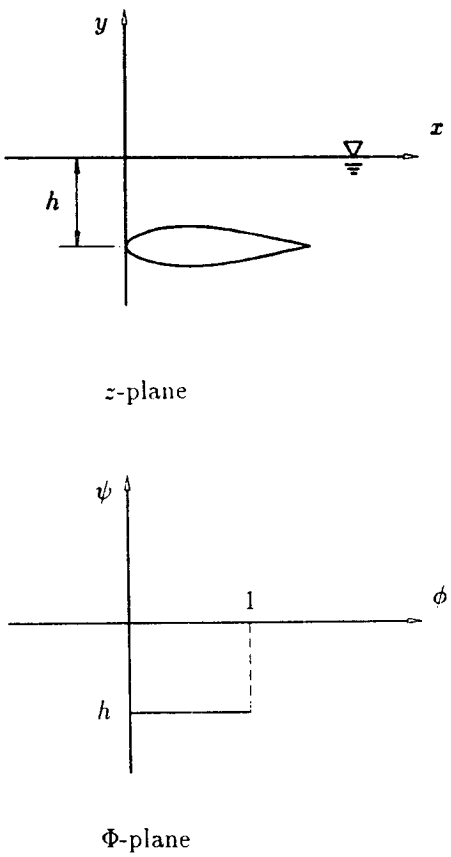

Figure 1. Co-ordinate systems.

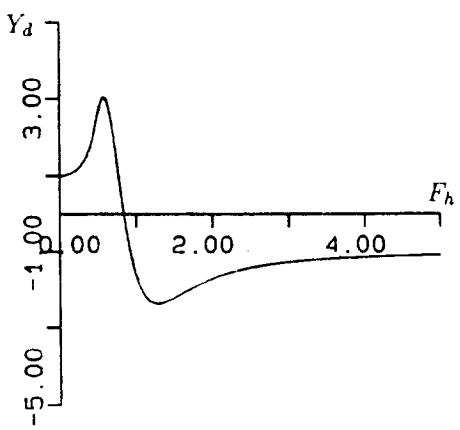

Figure 2. Lift of a submerged dipole Y_d vs. F_h.

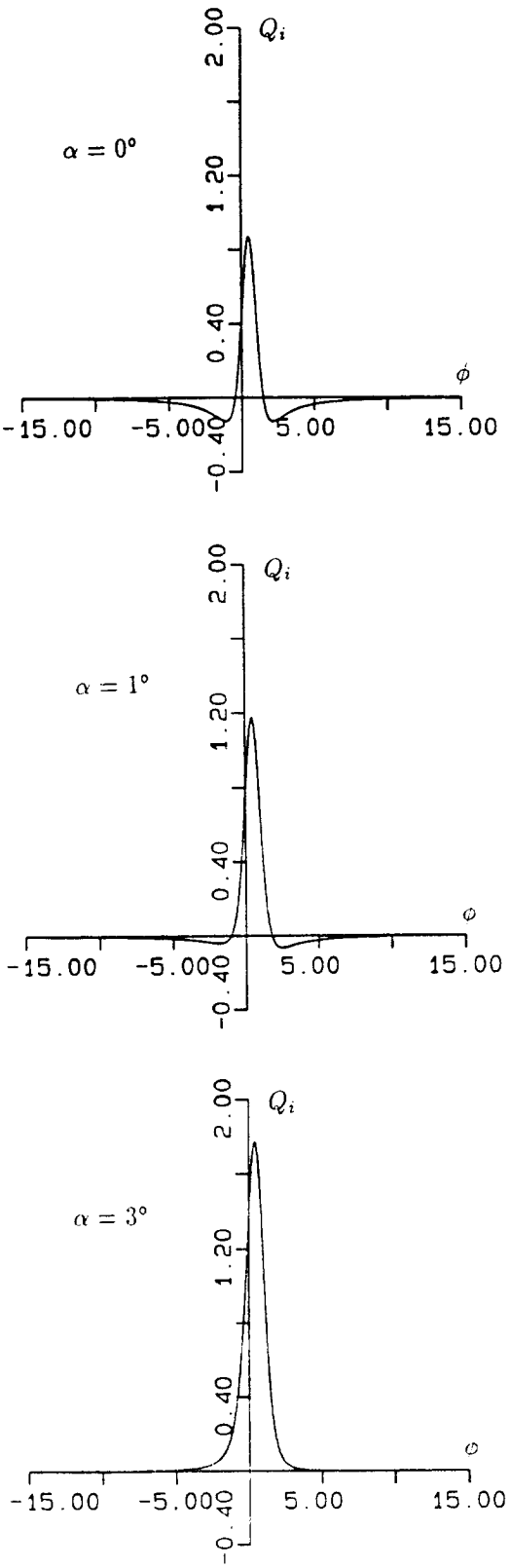

Figure 3. Q_i vs. ϕ where $F_n = 0.4, \delta = 0.2, h = 1.0$ for various attack angles.

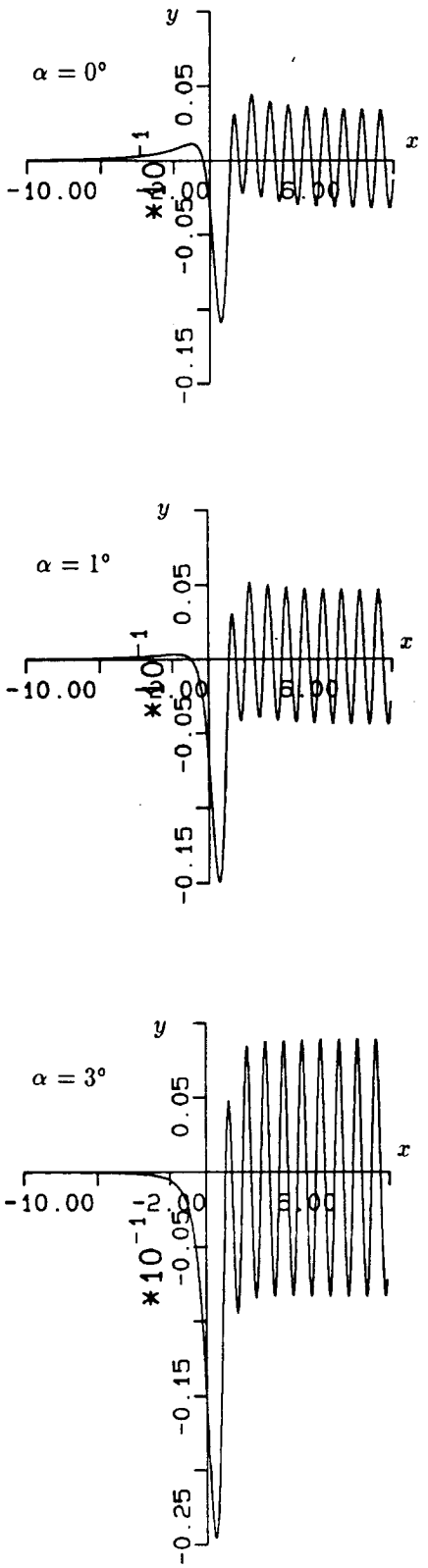

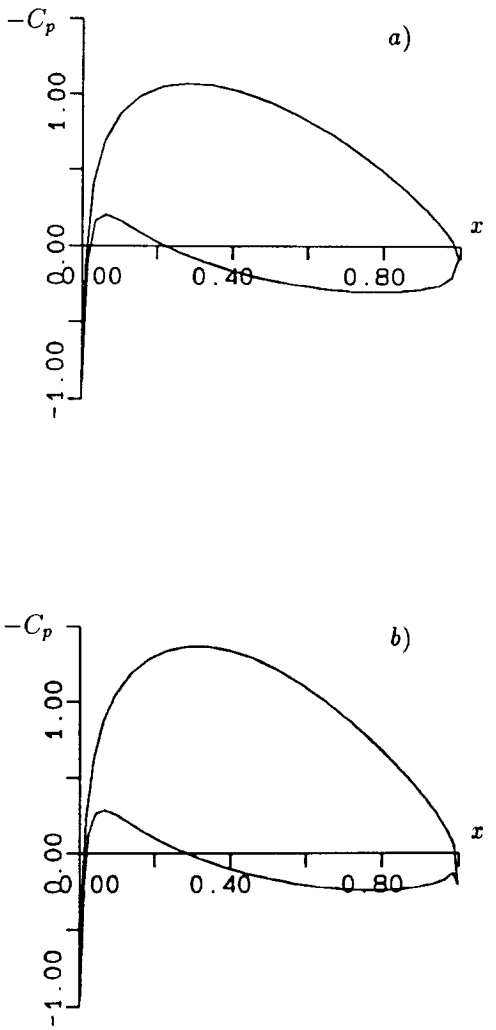

Figure 4. Free surface elevations where $F_n = 0.4, \delta = 0.2, h = 1.0$ for various attack angles.

Figure 5. C_p distribution on a cambered Joukowski hydrofoil a)in an infinite fluid, b) under the free surface, where $F_n = 0.4, h = 1.0, \alpha = 0°$.

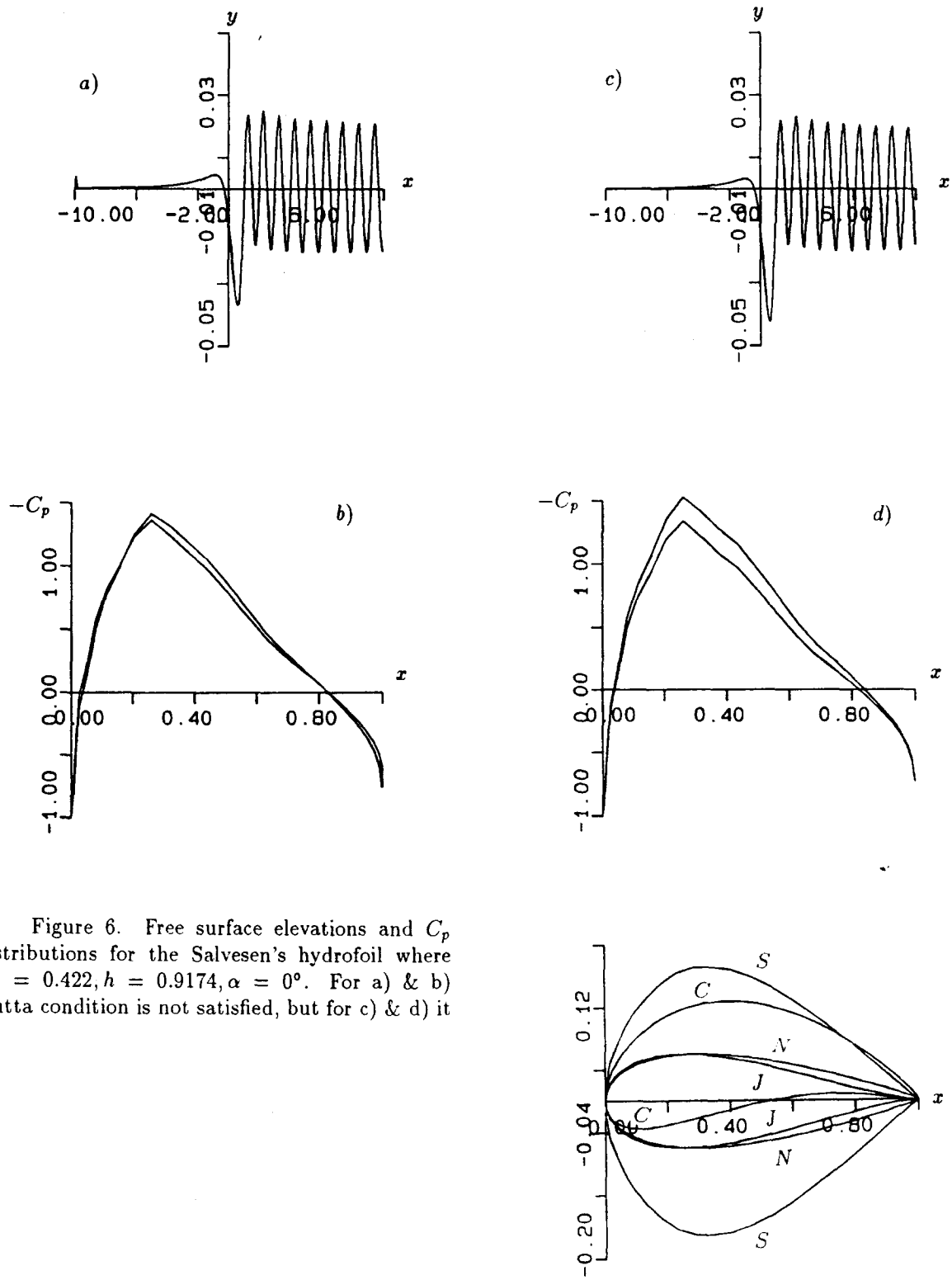

Figure 6. Free surface elevations and C_p distributions for the Salvesen's hydrofoil where $F_n = 0.422, h = 0.9174, \alpha = 0°$. For a) & b) Kutta condition is not satisfied, but for c) & d) it is.

Figure 7. Geometry of various foils, where S=Salvesen's foil, C=cambered Joukowski foil, N=foil of NACA 0012 section, J=symmetric Joukowski foil(12% thick).

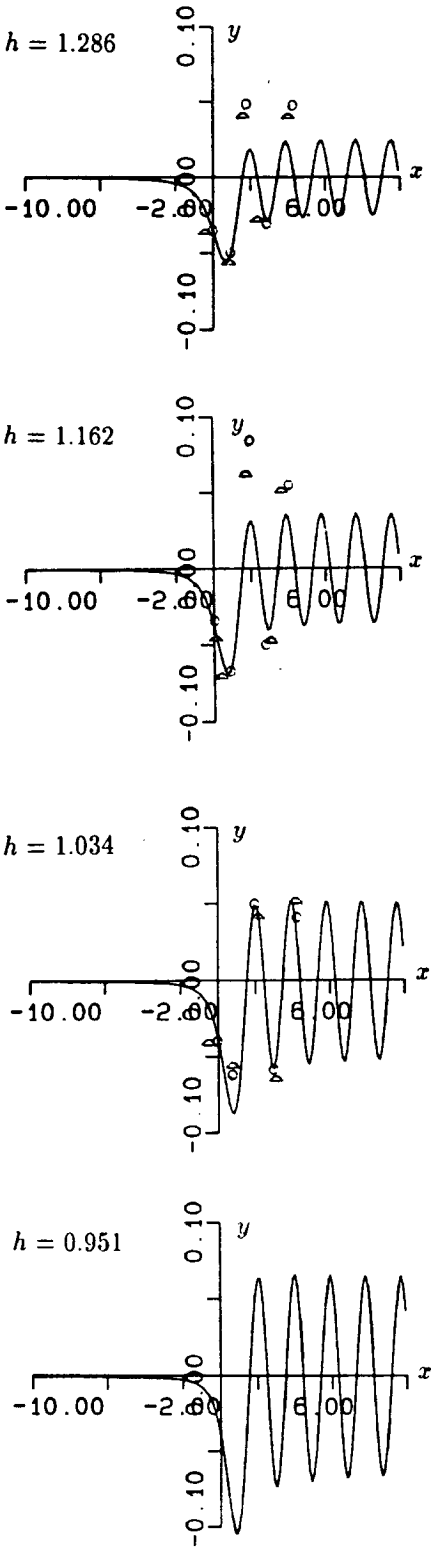

Figure 8. Free surface elevations for the foil of NACA 0012 section where $F_n = 0.567, \alpha = 5°$ for various h. Duncan's experimental data(▵) and Coleman's computational results(○) are shown together.

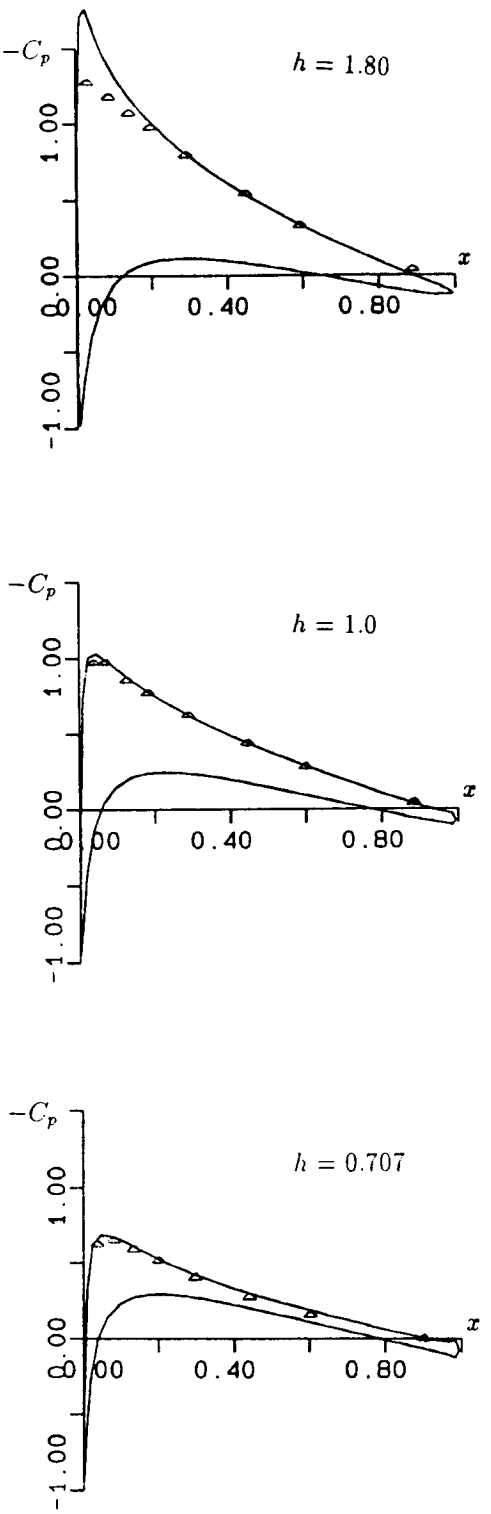

Figure 9. C_p distributions on the symmetric Joukowski hydrofoil of 12% thickness where $F_n = 0.95, \alpha = 5°$ for various h. Parkin et al.'s experimental data(▵) are shown together.